

## Domain morphology from $k$ -space spectroscopy of ferroelectric crystals

Uwe Voelker and Klaus Betzler\*

Fachbereich Physik, Universität Osnabrück, D-49069 Osnabrück, Germany

(Received 25 July 2006; published 18 October 2006)

A nonlinear-optical investigation technique for the domain structuring in ferroelectric crystals is reported. Noncollinear optical frequency doubling in a quasiphase-matched scheme allows for conclusions on the  $k$ -space representation of the domain morphology or—putting it in other terms—on the  $k$ -space representation of the correlation lengths ( $k$ -space spectroscopy). As an example, the ferroelectric-to-paraelectric phase transition of the relaxor ferroelectric strontium-barium niobate (SBN) is studied. One important result is that homogeneously poled crystals of SBN do *not* uniquely go through the phase transition as commonly assumed. Instead, the correlation length shows a characteristic anisotropic behavior in the phase-transition region.

DOI: [10.1103/PhysRevB.74.132104](https://doi.org/10.1103/PhysRevB.74.132104)

PACS number(s): 77.80.Dj, 42.65.Ky, 42.70.Mp, 77.84.Dy

For optical frequency doubling—second-harmonic generation (SHG)—usually *collinear* arrangements are used, i.e., the wave vectors of fundamental and harmonic waves are parallel to each other. Furthermore, so-called phase matching between fundamental and harmonic wave is adjusted in order to maximize the second-harmonic intensity—the momentum conservation law is fulfilled,

$$k_2 = 2k_1. \quad (1)$$

In Eq. (1),  $k_1$  and  $k_2$  are the wave vectors of the fundamental and of the harmonic wave, respectively, inside the nonlinear medium used for SHG. If two different fundamental wave polarizations are used, “ $2k_1$ ” should be replaced by “ $k_1 + k_1'$ .” The strong momentum conservation rule may also be fulfilled by adding an additional vector  $k_g$  which represents an appropriate spatial structure (quasiphase matching). The momentum conservation law then changes to

$$k_2 = 2k_1 + k_g. \quad (2)$$

Usually, quasiphase matching is achieved in regular domain structures<sup>1</sup> fabricated by periodic poling.

In general the three vectors involved in Eq. (2) need not be *collinear*, momentum conservation is a vectorial condition. As long as only three different vectors are involved, however, they have to be *coplanar*. The situation for an arbitrary plane is sketched in Fig. 1.

By a variation of  $\alpha$ , the length of  $k_g$ , i.e.,  $|k_g|$ , is varied according to the trigonometric relation:

$$|k_g| = (4|k_1|^2 + |k_2|^2 - 4|k_1||k_2|\cos\alpha)^{1/2}. \quad (3)$$

Thus a continuous  $|k_g|$  range between  $|k_2| - 2|k_1|$  (for  $\alpha = 0$ ) and  $|k_2| + 2|k_1|$  (for  $\alpha = \pi$ ) can be accessed. For the refractive indices of strontium-barium niobate and a fundamental wavelength  $\lambda_1 = 1064$  nm this means

$$1 \mu\text{m}^{-1} \leq |k_g| \leq 50 \mu\text{m}^{-1}, \quad (4)$$

corresponding to a spatial scale from approximately 100 nm to 5  $\mu\text{m}$ .

Rotating a crystal through an appropriate range of solid angles allows for a full inspection of the  $k_g$  density as a function of size and direction. This, in turn, presents a mea-

sure for the corresponding correlation lengths of these spatial inhomogeneities as a function of the crystallographic directions.

One special case of this kind of SHG is described in Ref. 2. The fundamental beam there is directed along the  $c$  axis of a strontium-barium niobate crystal. This leads to a cone of harmonic light around the fundamental beam which can be explained by the fact that only  $k_g$  vectors perpendicular the  $c$  axis are dominant contributors. It could be shown there that other known noncollinear scenarios for SHG or in combination with SHG are not able to explain the experimental results (for a more detailed discussion see Ref. 2).

Here we will use quasiphase-matched noncollinear SHG to study the domain morphology in strontium-barium niobate (SBN). SBN ( $\text{Sr}_x\text{Ba}_{1-x}\text{Nb}_2\text{O}_6$ ) crystals can be grown in a wide composition range spanning approximately  $x = 0.3 \dots 0.8$ .<sup>3,4</sup> A congruently melting composition, yielding crystals of high homogeneity, has been determined to be at  $x \approx 0.61$ .<sup>5</sup> At room temperature, undoped crystals of all compositions are ferroelectric with the tetragonal space group  $P4bm$ .<sup>6</sup> A phase transition into the paraelectric phase occurs at temperatures ranging from 20 to 220 °C depending on the composition.<sup>7</sup> The transition is relaxorlike, not at an expressed Curie temperature, instead spanning a so-called Curie range. Due to the crystal symmetry, two directions of the ferroelectric polarization are allowed, parallel and antiparallel to the crystallographic  $c$  axis. From the nonzero elements

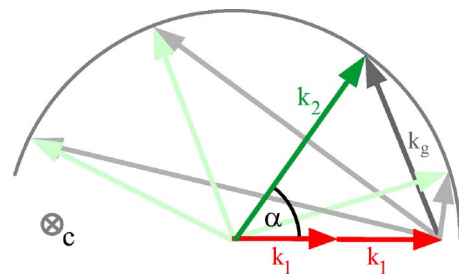


FIG. 1. (Color online) Phase matching condition for quasiphase-matched noncollinear second-harmonic generation.  $k_1$ : wave vector of fundamental beam,  $k_2$ : wave vector of second-harmonic light,  $k_g$ : wave vector representing a spatial structure in the crystal. The lengths of  $k_1$  and  $k_2$  are fixed, the length of  $k_g$  can be adjusted by varying  $\alpha$  accordingly.

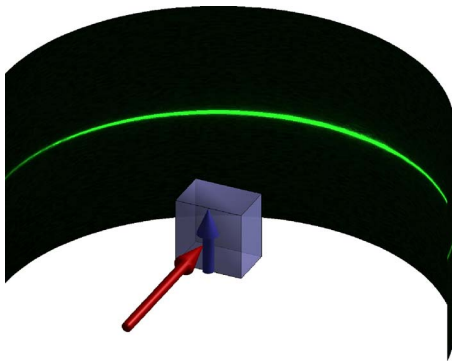


FIG. 2. (Color online) Principle of the measurements: a Nd:YAG laser beam (long arrow) is directed onto an SBN crystal in a direction perpendicular to the crystallographic  $c$  axis (short arrow). A photograph of the emitted SHG light pattern for an unpoled sample is shown on the screen.

in the nonlinear susceptibility tensor it can be deduced that generation of second-harmonic light is possible in all geometries where at least one of the three participating light waves has a polarization component parallel to the crystallographic  $c$  axis. In the paraelectric phase second-harmonic generation is prohibited due to its centric symmetry.

In our experiments we used optically homogeneous crystals grown from the congruently melting composition, as-grown unpoled or homogeneously poled. For the measurements we directed an unexpanded laser beam with low divergence (pulsed Nd:YAG at a wavelength of 1064 nm, 5 ns pulse length, 20 mJ pulse energy, 20 Hz repetition rate, 1.5 mm beam diameter) onto the samples (sample size  $a \times b \times c \approx 4 \times 4 \times 2$  mm<sup>3</sup>). To use the largest of the SHG tensor elements,  $d_{33}$ , the fundamental beam was polarized parallel to the  $c$  axis of the crystals. The principle of the experiment is sketched in Fig. 2.

Second-harmonic light is emitted only in the plane perpendicular to the  $c$  axis of the crystal. Taking into account the coplanarity of the process, this means that a noticeable density of  $k_g$  vectors is only found in this plane. Rotating the crystal around the  $c$  axis yielded no additional angular dependence. Therefore it can be concluded that the distribution of  $k_g$  vectors is isotropic in this plane. This is consistent with the agreed model for the unpoled ferroelectric phase of SBN,<sup>8–12</sup> namely a structure of 180° domains which are (anti) parallel to the crystallographic  $c$  axis. They must be assumed to be long in  $c$  direction and fractal-like shaped perpendicular to the  $c$  axis.<sup>13</sup> This means that the typical correlation length is large in  $c$  direction, whereas in all directions perpendicular to  $c$  the broad distribution of  $k_g$  vectors indicates a small correlation length, shorter than 1/40  $\mu\text{m}$ .

For quantitative measurements of the angular distribution of the SHG intensity we used the setup sketched in Fig. 3. The crystal is mounted in a temperature-controlled oven, the intensity of the emitted SHG light is measured by photomultipliers in combination with appropriate filters which suppress the fundamental laser light. The angular distribution of the SHG light is converted into the distribution of the  $|k_g|$  density using Eq. (3). All our measurements were restricted

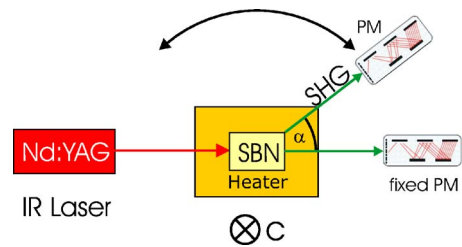


FIG. 3. (Color online) Setup for quantitative measurements: the infrared light hits the temperature-controlled crystal perpendicular to its  $c$  axis. The generated harmonic light is detected by two photomultipliers. One is rotated by a motorized stage around the crystal, the second one is mounted at a fixed angle of 0° with respect to the fundamental beam.

to the plane perpendicular to the  $c$  axis as in no experimental situation SHG light corresponding to  $k_g$  vectors outside this plane could be detected. This indicates that the correlation length in  $c$  direction is large—beyond our detection limits—throughout all experiments. Furthermore—as a rotation around the crystallographic  $c$  axis did not influence the signal intensity—the crystals were kept in a fixed angular position.

Figure 4 shows the intensity of the harmonic light as a function of  $|k_g|$  for a fixed temperature of 25 °C measured in the setup described. The measurements were made for two poling states of the crystal—unpoled as grown and homogeneously poled. Poling was achieved by applying an electric field of 200 V/mm to the crystal at a temperature of 150 °C, far above the Curie range for this composition, afterwards cooling slowly down to room temperature under applied field. The data for the unpoled SBN crystal are represented by gray dots: the intensity of the harmonic light is independent of  $|k_g|$  corresponding to the fractal-like shape, i.e., short correlation lengths perpendicular to the crystallographic  $c$  axis, as already discussed. In contrast to this the poled SBN crystal (black dots): the intensity of the harmonic light increases by several orders of magnitude when  $|k_g|$  approaches zero [due to Eqs. (3) and (4),  $|k_g|$  values below 1  $\mu\text{m}^{-1}$  are not accessible]. Together with the large coherence length in  $c$

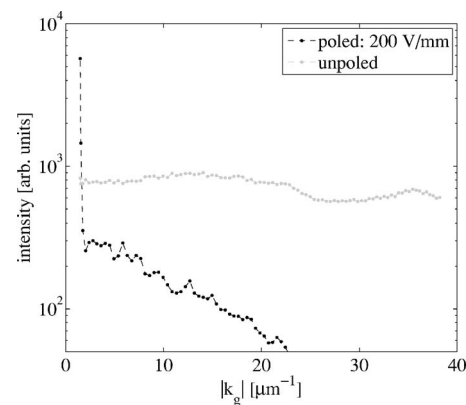


FIG. 4. Second-harmonic intensity as a function of  $|k_g|$  for directions perpendicular to the crystallographic  $c$  axis at a fixed temperature of 25 °C. Gray dots: unpoled SBN crystal, black dots: poled SBN crystal (data above 20  $\mu\text{m}^{-1}$  omitted due to low intensity).

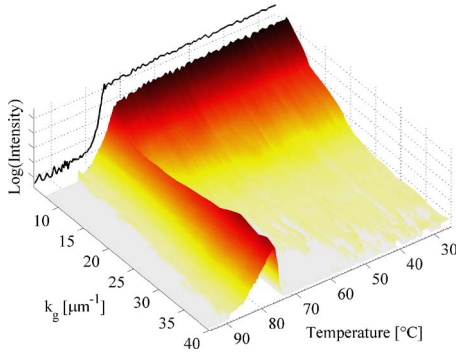


FIG. 5. (Color online) Temperature dependence of the  $|k_g|$  distribution for a homogeneously poled SBN sample heated up from room temperature. As a measure for the  $|k_g|$  density the intensity of the generated harmonic light is plotted (natural logarithmic scale). The broadening of the  $|k_g|$  distribution at temperatures in the Curie range indicates a corresponding modification in the domain morphology. The solid line denotes the harmonic intensity in forward direction (shifted down in scaling by one order of magnitude to fit into the picture).

direction already discussed, this corresponds to large correlation lengths in *all* directions, i.e., reflects the monodomain state achieved by the poling procedure. The low-intensity wing to higher  $|k_g|$  values seems to indicate higher order processes involving more than one  $k_g$ .

To study domain effects near the ferroelectric-to-paraelectric phase transition of SBN, the sample is heated at a rate of 0.012 K/s from room temperature up to temperatures well above the phase-transition range. During the heating cycle, the angular dependence of the emitted SHG intensity is continuously measured, thus the temperature dependence of the  $|k_g|$  distribution is yielded.

Unpoled samples show a broad distribution up to the phase-transition region, at temperatures above the phase transition the SHG intensity vanishes indicating the centric symmetry of the paraelectric phase.

Poled samples, however, show an unexpected temperature dependence which is depicted in Fig. 5. Up to temperatures just below the Curie range only small  $|k_g|$  values are found, indicating large correlation lengths in all directions, i.e., one large domain. In contrast to this, at temperatures in the Curie range the distribution of  $|k_g|$  values broadens considerably in the directions perpendicular to the *c* axis, indicating a distinct modification in the domain morphology. The measurements show that this modification persists over a comparably broad temperature range. At higher temperatures, due to the transition into the unpolar paraelectric phase, second-harmonic generation vanishes completely. On cooling, the sample shows the typical behavior experienced for unpoled samples.

Up to now such a modification of the domain morphology in the Curie range had only been found near domain boundaries of unpoled samples of Cerium-doped SBN which were investigated by piezoelectric force microscopy.<sup>13</sup> However, in these measurements it could be only shown that a fractal-like filamentation occurs at the surface of the crystals. With this type of *k*-space spectroscopy we can prove that this restructuring also occurs in the bulk of the crystals and, fur-

thermore, that the restructured microregions are—at least partly—polar throughout the Curie range.

Our results strongly point to an interesting model for the phase transition in SBN. Cooling the samples in a sufficiently high electric field parallel to the polar axes leads to a monodomain ferroelectric state. On heating, the monodomain state persists up to the Curie range. In the Curie range, however, the monodomain state collapses into a polar cluster state with highly anisotropic correlation lengths, large in *c* direction but small perpendicular to *c*. Such an anisotropic characteristic had earlier been proposed by Huang *et al.*,<sup>14</sup> however, no direct proof could be given. When the crystal is cooled down through the phase-transition region without an electric field applied, the broad uniform distribution of correlation lengths perpendicular to the polar axis combined with the large correlation length in *c* direction is sustained down to temperatures far below the phase transition. This refers to a freezing of the polar cluster state as presumed, e.g., by Dec *et al.*<sup>15</sup>

To compare the two low-temperature states—field cooled (FC) and zero-field cooled (ZFC)—we derived the critical exponent  $\beta$  from our measurements. This exponent is used to characterize the class of the phase transition. In the vicinity of the phase transition, the order parameter can be described by a generalized exponential law with  $\beta$  being the exponent. For a ferroelectric, the order parameter is the spontaneous polarization *P*, its dependence on temperature *T* is described by

$$P(T) = P_0 [1 - (T + 273)/(T_C + 273)]^\beta. \quad (5)$$

The tensor elements  $d_{ik}$  of the second-harmonic susceptibility tensor are in good approximation proportional to *P*. The second harmonic intensity, in turn, is proportional to the square of the effective *d*, which is an appropriate weighted sum of the  $d_{ik}$ . Thus, for the temperature dependence of the second harmonic intensity, we obtain

$$I_{\text{SHG}}(T) = I_{\text{SHG},0} [1 - (T + 273)/(T_C + 273)]^{2\beta}. \quad (6)$$

Evaluations of pyroelectric measurements have shown<sup>16</sup> that—for SBN—Eq. (5) describes the experimental results excellently between  $T_C - 20$  K and  $T_C$ . Therefore we calculated the fit of Eq. (6) to the experimental data using this broad temperature range, too. The parameters yielded from the fit are  $T_C = 75.8$  °C for both cases and  $\beta = 0.09 \pm 0.03$  for the FC state,  $\beta = 0.10 \pm 0.03$  for the ZFC state, respectively. The agreement between the two values of  $\beta$  shows that the phase transitions—field cooled and zero-field cooled—belong to the same universality class. A strong indication that by field cooling only negligible additional stress is imposed on the crystal.

The value of  $\beta$  found is a strong hint towards a three-dimensional random-field Ising model<sup>17</sup> for the explanation of the phase transition in pure SBN. The interesting fact is that—despite the different behavior of the correlation lengths—both, FC and ZFC states obey identical parameters. The three-dimensional (3D) random-field Ising model thus turns out to be a common model for the relaxor phase transition in SBN—not only for crystals with appropriately chosen special dopants.<sup>18</sup>

In conclusion, we have reported on a special way of  $k$ -space spectroscopy in ferroelectric crystals. The technique utilizes a mechanism for the noncollinear generation of second-harmonic light in polar crystals which can be described as *noncollinear quasiphase matching* where the necessary additional  $k$ -vector  $k_g$  is taken from the Fourier representation of the domain geometry or—correspondingly—of the correlation lengths. Applying this technique, we could directly probe the distribution of correlation lengths in the phase transition region of a ferroelectric. For undoped strontium barium niobate we could show that field cooling leads to a monodomain ferroelectric state with large correlation lengths in all directions. Cooling from the paraelectric state with zero electric field, however, yields a low temperature

state with a highly anisotropic distribution of the correlation lengths—a frozen polar cluster state with a large correlation length in the direction of the polar axis. Both low temperature states are characterized by an identical critical exponent  $\beta$  and an identical characteristic temperature  $T_C$ . The value of the critical exponent  $\beta$  strongly hints to a 3D random-field Ising model governing the ferroelectric-paraelectric phase transition in strontium barium niobate.

We are indebted to Michael Ulex for growing the crystals used through the measurements. Support from the Graduate College *Nonlinearities of Optical Materials*, financed by the Deutsche Forschungsgemeinschaft and the Federal State of Niedersachsen, is gratefully acknowledged.

---

\*Electronic address: Klaus.Betzler@uos.de

- <sup>1</sup>J. A. Armstrong, N. Bloembergen, J. Ducuing, and P. S. Pershan, *Phys. Rev.* **127**, 1918 (1962).
- <sup>2</sup>A. R. Tunyagi, M. Ulex, and K. Betzler, *Phys. Rev. Lett.* **90**, 243901 (2003).
- <sup>3</sup>A. A. Ballman and H. Brown, *J. Cryst. Growth* **1**, 311 (1967).
- <sup>4</sup>J. C. Brice, O. F. Hill, P. A. C. Whiffin, and J. A. Wilkinson, *J. Cryst. Growth* **10**, 133 (1971).
- <sup>5</sup>K. Megumi, N. Nagatsuma, Y. Kashiwada, and Y. Furuhashi, *J. Mater. Sci.* **11**, 1583 (1976).
- <sup>6</sup>P. B. Jameson, S. C. Abrahams, and J. L. Bernshtein, *J. Chem. Phys.* **42**, 5048 (1968).
- <sup>7</sup>C. David, T. Granzow, A. Tunyagi, M. Wöhlecke, T. Woike, K. Betzler, M. Ulex, M. Imlau, and R. Pankrath, *Phys. Status Solidi A* **201**, R49 (2004).
- <sup>8</sup>G. Fogarty, B. Steiner, M. Cronin-Golomb, U. Laor, M. H. Garrett, J. Martin, and R. Uhrin, *J. Opt. Soc. Am. B* **13**, 2636 (1996).
- <sup>9</sup>S. Kawai, T. Ogawa, H. S. Lee, R. C. DeMattei, and R. S. Feigelson, *Appl. Phys. Lett.* **73**, 768 (1998).
- <sup>10</sup>Y. G. Wang, W. Kleemann, T. Woike, and R. Pankrath, *Phys. Rev. B* **61**, 3333 (2000).
- <sup>11</sup>W. Kleemann, P. Licinio, T. Woike, and R. Pankrath, *Phys. Rev. Lett.* **86**, 6014 (2001).
- <sup>12</sup>J. J. Romero, D. Jaque, J. García Solé, and A. A. Kaminskii, *Appl. Phys. Lett.* **78**, 1961 (2001).
- <sup>13</sup>P. Lehnen, W. Kleemann, T. Woike, and R. Pankrath, *Phys. Rev. B* **64**, 224109 (2001).
- <sup>14</sup>W. H. Huang, D. Viehland, and R. R. Neurgaonkar, *J. Appl. Phys.* **76**, 490 (1994).
- <sup>15</sup>J. Dec, W. Kleemann, V. Bobnar, Z. Kutnjak, A. Levstik, R. Pirc, and R. Pankrath, *Europhys. Lett.* **55**, 781 (2001).
- <sup>16</sup>T. Granzow, T. Woike, M. Wöhlecke, M. Imlau, and W. Kleemann, *Phys. Rev. Lett.* **92**, 065701 (2004).
- <sup>17</sup>H. Rieger, *Phys. Rev. B* **52**, 6659 (1995).
- <sup>18</sup>W. Kleemann, J. Dec, P. Lehnen, R. Blinc, B. Zalar, and R. Pankrath, *Europhys. Lett.* **57**, 14 (2002).